www.kidney-international.org basic research

Augmentative effects of leukemia inhibitory factor reveal a critical role for TYK2 signaling in vascular calcification



OPEN

loana Alesutan¹, Mehdi Razazian¹, Trang T.D. Luong¹, Misael Estepa², Lakmi Pitigala¹, Laura A. Henze², Jakob Obereigner¹, Gregor Mitter¹, Daniel Zickler³, Mirjam Schuchardt^{3,4}, Christine Deisl¹, Manousos Makridakis⁵, Can Gollmann-Tepeköylü⁶, Andreas Pasch^{1,7}, Daniel Cejka⁸, Susanne Suessner⁹, Marlies Antlanger¹⁰, Bernhard Bielesz¹¹, Mathias Müller¹², Antonia Vlahou⁵, Johannes Holfeld⁶, Kai-Uwe Eckardt³ and Jakob Voelkl^{1,3,13}

¹Institute for Physiology and Pathophysiology, Johannes Kepler University Linz, Linz, Austria; ²Department of Internal Medicine and Cardiology, Corporate Member of Freie Universität Berlin and Humboldt Universität zu Berlin, Berlin, Germany; ³Department of Nephrology and Medical Intensive Care, Charité–Universitätsmedizin Berlin, Corporate Member of Freie Universität Berlin and Humboldt Universität zu Berlin, Berlin, Germany; ⁴Faculty of Medicine, Medical School Berlin, Berlin, Germany; ⁵Center of Systems Biology, Biomedical Research Foundation Academy of Athens, Athens, Greece; ⁶Department for Cardiac Surgery, Medical University of Innsbruck, Innsbruck, Austria; ⁷Calciscon AG, Biel, Switzerland; ⁸Internal Medicine III–Nephrology, Transplantation Medicine, Rheumatology, Ordensklinikum Linz, Linz, Austria; ⁹Red Cross Transfusion Service of Upper Austria, Linz, Austria; ¹⁰Department of Internal Medicine 2, Kepler University Hospital and Johannes Kepler University, Linz, Austria; ¹¹Division of Nephrology and Dialysis, Department of Medicine III, Medical University of Vienna, Vienna, Austria; ¹²Institute of Animal Breeding and Genetics, University of Veterinary Medicine Vienna, Vienna, Austria; and ¹³DZHK (German Centre for Cardiovascular Research), Partner Site Berlin, Berlin, Germany

Medial vascular calcification in chronic kidney disease (CKD) involves pro-inflammatory pathways induced by hyperphosphatemia. Several interleukin 6 family members have been associated with pro-calcific effects in vascular smooth muscle cells (VSMCs) and are considered as therapeutic targets. Therefore, we investigated the role of leukemia inhibitory factor (LIF) during VSMC calcification. LIF expression was found to be increased following phosphate exposure of VSMCs. LIF supplementation aggravated, while silencing of endogenous LIF or LIF receptor (LIFR) ameliorated the pro-calcific effects of phosphate in VSMCs. The soluble LIFR mediated antagonistic effects towards LIF and reduced VSMC calcification. Mechanistically, LIF induced phosphorylation of the non-receptor tyrosineprotein kinase 2 (TYK2) and signal transducer and activator of transcription-3 (STAT3) in VSMCs. TYK2 inhibition by deucravacitinib, a selective, allosteric oral immunosuppressant used in psoriasis treatment, not only blunted the effects of LIF, but also interfered with the pro-calcific effects induced by phosphate. Conversely, TYK2 overexpression aggravated VSMC calcification. Ex vivo calcification of mouse aortic rings was ameliorated by Tyk2 pharmacological inhibition and genetic deficiency. Cholecalciferol-induced vascular calcification in mice was improved by Tyk2 inhibition

Correspondence: Jakob Voelkl, Institute for Physiology and Pathophysiology, Johannes Kepler University Linz, Krankenhausstrasse 5, 4020 Linz, Austria. E-mail: jakob.voelkl@jku.at

Received 4 August 2023; revised 28 June 2024; accepted 10 July 2024; published online 30 July 2024

and in the Tyk2-deficient mice. Similarly, calcification was ameliorated in Abcc6/Tyk2-deficient mice after adenine/high phosphorus-induced CKD. Thus, our observations indicate a role for LIF in CKD-associated vascular calcification. Hence, the effects of LIF identify a central pro-calcific role of TYK2 signaling, which may be a future target to reduce the burden of vascular calcification in CKD.

Kidney International (2024) **106,** 611–624; https://doi.org/10.1016/j.kint.2024.07.011

KEYWORDS: chronic kidney disease; leukemia inhibitory factor; STAT3; TYK2; vascular calcification; vascular smooth muscle cells

Copyright © 2024, International Society of Nephrology. Published by Elsevier Inc. This is an open access article under the CC BY license (http://creativecommons.org/licenses/by/4.0/).

Translational Statement

Inhibition of pro-inflammatory pathways, such as interleukin 6 (IL-6), is emerging as a putative therapeutic strategy to counter the excessive cardiovascular mortality in chronic kidney disease (CKD). This study suggests that dysregulation of the IL-6 family member leukemia inhibitory factor is involved in vascular smooth muscle cell calcification. Mechanistic experiments identified the tyrosine-protein kinase (TYK) 2 of the Janus kinase (JAK) family as a central regulator during vascular calcification. Because TYK2 inhibition with deucravacitinib is feasible with an improved safety profile over other JAK/signal transducer and activator of transcription inhibitors, it might be a promising and translatable strategy to reduce the burden of calcification in patients with CKD.

atients with chronic kidney disease (CKD) are prone to develop hyperphosphatemia, which is associated with medial vascular calcification (VC). These calcifications are associated with cardiovascular mortality, and no broadly available therapeutic approaches are established. VC involves active cell-mediated processes, where vascular smooth muscle cells (VSMCs) may alter their environment to favor mineral deposition on phosphate exposure.²

The cellular reprogramming toward procalcific VSMCs is orchestrated by various transcription factors, such as osterix or core-binding factor subunit α -1 (CBFA1), also known as runt-related transcription factor 2 (RUNX2). In VC, multiple signaling pathways may converge on CBFA1, which upregulates the expression of the mineralization regulator tissue-nonspecific alkaline phosphatase (ALPL). 5,6

Various inflammatory transmitters can induce a calcific phenotype of VSMCs.² A prominent role thereby is attributed to the interleukin 6 (IL-6) family. Procalcific effects were shown for oncostatin M,7 but special focus has been given to IL-6.8 In patients undergoing dialysis, IL-6 is associated with coronary calcification and mortality.9 IL-6 inhibition reduced inflammatory biomarkers in patients with CKD.¹⁰ IL-6 can activate procalcific pathways in VSMCs, such as signal transducer and activator of transcription (STAT) 3 of the STAT protein family. 11 STAT3 upregulates CBFA1 expression and thereby augments VSMC calcification. 11 Other procalcific mediators may also transmit their effects via STAT3, such as interleukin 29¹² or endothelial microparticles. 13 STAT3 can be activated by the Janus kinase (JAK) family of receptor-associated tyrosine kinase, in which the nonreceptor tyrosine-protein kinase 2 (TYK2) can provide signal amplification.¹⁴ However, the JAK/STAT effects and pathways are often cell type specific 14 and not well defined in VC.

Another member of the IL-6 family is leukemia inhibitory factor (LIF).15 LIF signals through several pathways activating STAT1 and STAT3. 15 LIF signaling is mediated by a receptor complex of glycoprotein 130 (GP130) and LIF receptor (LIFR).¹⁶ Interestingly, both GP130 and LIFR are found in a soluble form and have antagonistic effects.¹⁷ Soluble LIFR has been detected in human plasma, 18 and the main production of soluble LIFR in mice has been attributed to the liver. 19 LIF itself has been associated with pleiotropic effects that vary in a cell-, tissue-, and contextdependent manner.²⁰ Vasculoprotective effects of LIF were discussed, because LIF infusion slows the progression of atherosclerotic lesions in rabbits.²¹ Furthermore, LIF can induce inducible nitric oxide synthase activation and inhibit neointima formation.²² A complex role for LIF and LIFR in bone remodeling has been discussed.²³ Parathyroid hormone upregulates the expression of LIF in osteoblasts.²⁴ Although inconsistent findings were reported, LIF is upregulated in kidney fibrosis, where LIF inhibition counteracts the fibrotic response.²⁵ In patients with coronavirus disease 2019 (COVID-19), LIF concentrations were negatively correlated with kidney function.²⁶

Therefore, this study investigated LIF as a potentially relevant signaling pathway in CKD. This identified a novel procalcific role of LIF in VSMC calcification. Mechanistically, these effects identified a critical role for TYK2 in the procalcific STAT signaling of VSMCs and suggested a therapeutic benefit of TYK2 blockade by deucravacitinib in CKD.

METHODS Cell culture

Primary human aortic smooth muscle cells were routinely cultured, as described previously,^{27,28} and treated as described in the Supplementary Material. Primary human osteoblast (HOb) culture and treatments are described in the Supplementary Material. LIF concentrations and extracellular vesicle release in conditioned culture medium were determined using the Bio-Plex Pro Human Cytokine LIF Set (Bio-Rad) and nanoflow analyzer (NanoFCM), respectively. Alkaline phosphatase (ALP) activity was determined by using a colorimetric ALP assay (Abcam), STAT1 and STAT3 activities were determined in nuclear extracts by using a colorimetric STAT transcription factor assay (Abcam), and T-cell factor/lymphoid enhancer factor (TCF/LEF)—dependent transcriptional activity was determined by a luciferase reporter assay (Qiagen).

Animal experiments

Animal experiments were approved by local authorities (Bundesministerium für Bildung, Wissenschaft und Forschung - BMBWF). Calcification was induced by cholecalciferol injection^{27,29} in C57Bl/6 mice receiving either vehicle or 15 mg/kg BMS-986165 as well as Tyk2-deficient mice (Tyk2^{-/-}) and corresponding wild-type mice (Tyk2^{+/+}).³⁰ ATP-binding cassette subfamily C member 6 (Abcc6)–deficient Tyk2^{-/-} and Tyk2^{+/+} mice were fed intermittently with an adenine/high-phosphorus diet. Serum analysis was performed by a photometric method (FUJI Dri-Chem Nx700) and by enzyme-linked immunosorbent assays. Distal femora of mice were analyzed by *ex vivo* micro–computed tomography imaging. Isolated aortic rings from mice were cultured and treated with 1.6 mM phosphate with/without 100 nM BMS-986165.

RNA isolation and reverse transcription-polymerase chain reaction

Total RNA was isolated by using Trizol reagent (Fisher Scientific). cDNA synthesis was performed with oligo(dT)₁₂₋₁₈ primers and Superscript III Reverse Transcriptase (Fisher Scientific) and reverse transcription–polymerase chain reaction with iQ Sybr Green Supermix (Bio-Rad). Primers are described in the Supplementary Material. Relative mRNA fold changes were calculated by the $2^{-\Delta\Delta Ct}$ method using glyceraldehyde-3-phosphate dehydrogenase as housekeeping gene.

Western blot analysis and immunofluorescence staining

Proteins were isolated with Pierce IP lysis buffer (Fisher Scientific) and separated on sodium dodecylsulfate–polyacrylamide gel electrophoresis gels. Membranes were incubated with primary antibodies described in the Supplementary Material. Bands were quantified using ImageJ software. Data are shown as the ratio of phosphorylated to total protein to glyceraldehyde-3-phosphate dehydrogenase and of total protein to glyceraldehyde-3-phosphate dehydrogenase, normalized to the control group. ^{29,31}

Cells and aortic sections were incubated with primary anti-RUNX2 (Cell Signaling) or anti-phosphorylated STAT3 (Tyr⁷⁰⁵; Cell Signaling) antibodies and then with Alexa488-conjugated (Molecular Probes) or Alexa647-conjugated (Molecular Probes) antibodies. Images were acquired on a Nikon Ti-2 microscope equipped with a Clarity Confocal Unit (Aurox).

Calcification analysis

Cells were incubated with OsteoSense 680EX (Perkin Elmer) and imaged with ChemiDoc MP (Bio-Rad Laboratories)³² or were fixed with 4% paraformaldehyde/phosphate-buffered saline and stained with 2% Alizarin red (pH 4.5). Human aortic smooth muscle cells and aortic tissues were decalcified, and calcium content was quantified with the QuantiChrom Calcium assay kit (BioAssay Systems). Data are shown normalized to total protein concentration (Bradford Assay) and to the control group.

Statistical analysis

Data are shown as scatter dot plots and means \pm SEM. Normality was determined by Shapiro-Wilk test, and statistical testing was performed using t test, Mann-Whitney U test, or Wilcoxon test. For >2 groups, 1-way analysis of variance with Tukey test or Games-Howell test and Kruskal-Wallis test with Steel-Dwass test were used. P < 0.05 was considered statistically significant.

Detailed methods are described in the Supplementary Methods.

RESULTS

LIF-augmented calcification of VSMCs

To investigate the putative role of LIF in the calcification of VSMCs, primary human aortic VSMCs were exposed to the phosphate donor β-glycerophosphate. Phosphate exposure significantly upregulated the mRNA expression of *LIF* and its receptors *LIFR* and *GP130* in VSMCs (Figure 1a–c). The mRNA levels and protein abundance of *LIFR* in VSMCs increased after 30 minutes of treatment (Supplementary Figure S1). Furthermore, LIF release in the medium was increased in phosphate-treated VSMCs (Figure 1d). To determine a functional relevance, VSMCs were treated with recombinant human LIF protein, which increased CBFA1 nuclear localization (Figure 1e) and the protein expression of CBFA1 and osterix (Supplementary Figure S2) as well as extracellular vesicle release (Figure 1f). Most important, LIF

supplementation aggravated calcification of VSMCs exposed to calcification medium (Figure 1g-i). LIF exposure was sufficient to upregulate the mRNA expression of *CBFA1* and *ALPL* as well as ALP activity and further aggravated the effects of phosphate in VSMCs (Figure 1j-l).

LIF inhibition ameliorated calcification of VSMCs

To confirm the response of VSMCs toward exogenous LIF, the endogenous expression of the receptors LIFR and GP130 was silenced using small interfering RNA (Supplementary Figure S3A and B). These knockdowns abrogated the LIF-induced increase of *CBFA1* and *ALPL* mRNA expression (Figure 2a and b). The role of LIF in VSMC calcification was investigated by silencing of endogenous LIF (Supplementary Figure S3C). LIF knockdown ameliorated the phosphate-induced increase of *CBFA1* and *ALPL* mRNA expression as well as calcification of VSMCs (Figure 2c–f). Furthermore, silencing of either LIFR or GP130 ameliorated the stimulating effects of phosphate on *CBFA1* and *ALPL* mRNA expression (Supplementary Figure S4).

Further experiments addressed a putative role of soluble LIFR as an inhibitor of the procalcific effects of LIF. As shown in Figure 3a and b, addition of exogenous recombinant human LIFR protein could prevent the increase in CBFA1 and ALPL mRNA expression in VSMCs after LIF treatment. Treatment with recombinant human GP130 protein could, apparently, not replicate the effects, but in additional experiments, a dose-dependent inhibition of these LIF-induced effects by GP130 was observed (Supplementary Figure S5). In the absence of LIF, LIFR or GP130 supplementation did not show any effects (Supplementary Figure S6A and B). Further experiments explored the effects of soluble LIFR on VSMC calcification. Addition of recombinant human LIFR or GP130 was able to ameliorate the increased mRNA expression of osteogenic markers induced by phosphate in VSMCs (Figure 3c and d). Furthermore, calcification of VSMCs was blunted by additional treatment with recombinant human LIFR (Figure 3e and f).

LIF induced a TYK2-STAT pathway to mediate procalcific effects

Next, the mechanisms underlying the procalcific effects of LIF were explored. LIF exposure of VSMCs led to a rapid increase in TYK2 and STAT3 phosphorylation (Figure 4a–d; Supplementary Figure S7A and B). In addition, we observed an increase in STAT1 phosphorylation following LIF treatment (Supplementary Figure S7C). TYK2 was apparently required to increase STAT3 activation in response to LIF, because additional treatment with the TYK2 inhibitor BMS-986165 (deucravacitinib) prevented the LIF-induced STAT3 phosphorylation and nuclear localization as well as activity (Figure 4e–h; Supplementary Figure S8A). Similarly, STAT1 phosphorylation and activity were increased by LIF, effects ameliorated in the presence of BMS-986165 (Supplementary Figure S8B and C). Moreover, silencing of TYK2, STAT1, or STAT3 prevented the LIF-induced increase of CBFA1 and

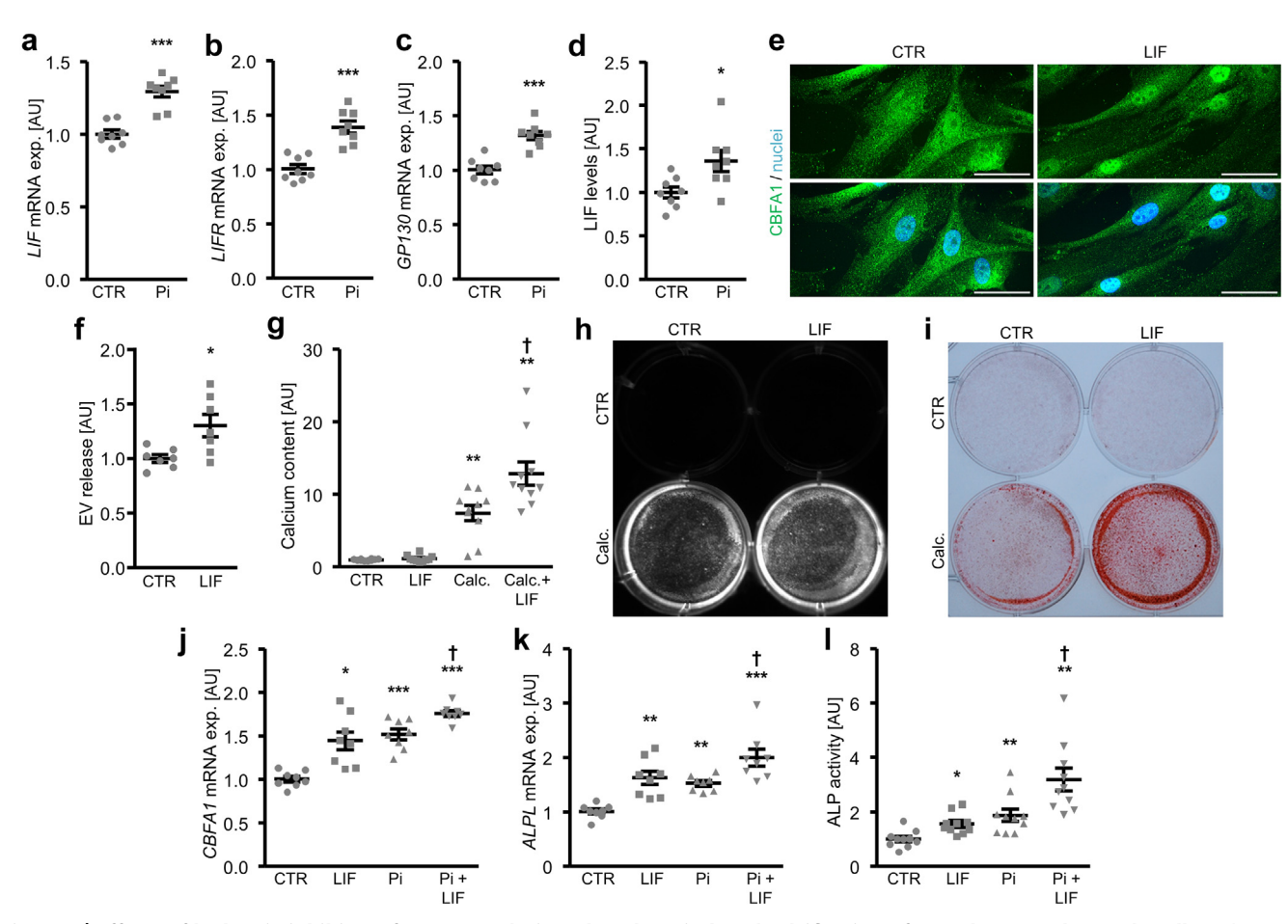


Figure 1 | Effects of leukemia inhibitory factor (LIF) during phosphate-induced calcification of vascular smooth muscle cells. Relative mRNA expression (exp.; n=8) of (a) LIF, (b) LIFR, and (c) GP130 in human aortic smooth muscle cells (HAoSMCs) treated for 24 hours with β-glycerophosphate (Pi). (d) Normalized LIF concentrations (n=8) in conditioned culture medium of HAoSMCs treated for 30 minutes with Pi. (e) Core-binding factor subunit α-1 (green) and nuclei (blue) shown by confocal imaging in HAoSMCs treated for 6 hours with recombinant human LIF protein. Bar = 50 μm. (f) Normalized extracellular vesicle (EV) release (n=7) in conditioned culture medium of HAoSMCs treated for 48 hours with recombinant human LIF protein. (g) Normalized calcium content (n=10) and calcification detected by (h) Osteosense fluorescence imaging or (i) Alizarin red staining in HAoSMCs treated for 11 days with recombinant human LIF protein with/without calcification medium (Calc.). Calcified areas: white pseudocolor/red staining. Relative mRNA expression (n=8) of (j) CBFA1 and (k) ALPL as well as (l) normalized alkaline phosphatase (ALP) activity (n=10) in HAoSMCs treated for 24 hours and 7 days, respectively, with recombinant human LIF protein with/without Pi. *P < 0.05, **P < 0.01, ***P < 0.001 versus control (CTR); †P < 0.05 versus Calc./Pi (unpaired 2-tailed t test for [a-d,f]; Kruskal-Wallis with Steel-Dwass test for [g] and [l]; and 1-way analysis of variance with Games-Howell test for [j] and with Tukey honestly significant difference test for [k]). AU, arbitrary unit.

ALPL mRNA expression in VSMCs (Supplementary Figure S9 and S10). Both LIF and phosphate treatment increased Wingless-integrated (WNT)/β-catenin pathway activity, whereas BMS-986165 blunted the phosphate-induced increase (Supplementary Figure S11). Silencing of endogenous LIF ameliorated the phosphate-induced increase of *IL6* mRNA expression, but not of *TNFA* or *IL1B*. None of their inhibition blocked the upregulation of *CBFA1* or *ALPL* induced by LIF (Supplementary Figure S12). Similar observations were made on early growth response factor-1 (Supplementary Figure S13).

TYK2 exerted a central role during VSMC calcification

As TYK2 emerged as a druggable signaling component in VSMC calcification, its role was investigated during

phosphate exposure. Increased phosphorylation of TYK2 and STAT3 was observed after phosphate exposure of VSMCs (Figure 5a–d; Supplementary Figure S14A and B). For STAT1, phosphate induced an increase of total protein abundance (Supplementary Figure S14C). On the basis of these observations, we investigated whether inhibition of this pathway could ameliorate the procalcific effects of phosphate. After phosphate exposure, TYK2 inhibition by BMS-986165 and the STAT inhibitor fludarabine or stattic ameliorated the phosphate-induced *CBFA1* and *ALPL* mRNA expression (Figure 5e and f). In the absence of phosphate, no effects of inhibitors were observed (Supplementary Figure S6C and D). TYK2 inhibition by BMS-986165 blunted the phosphate-induced increase of STAT3 activity (Figure 5g), and similar observations were made for STAT1 activity (Supplementary

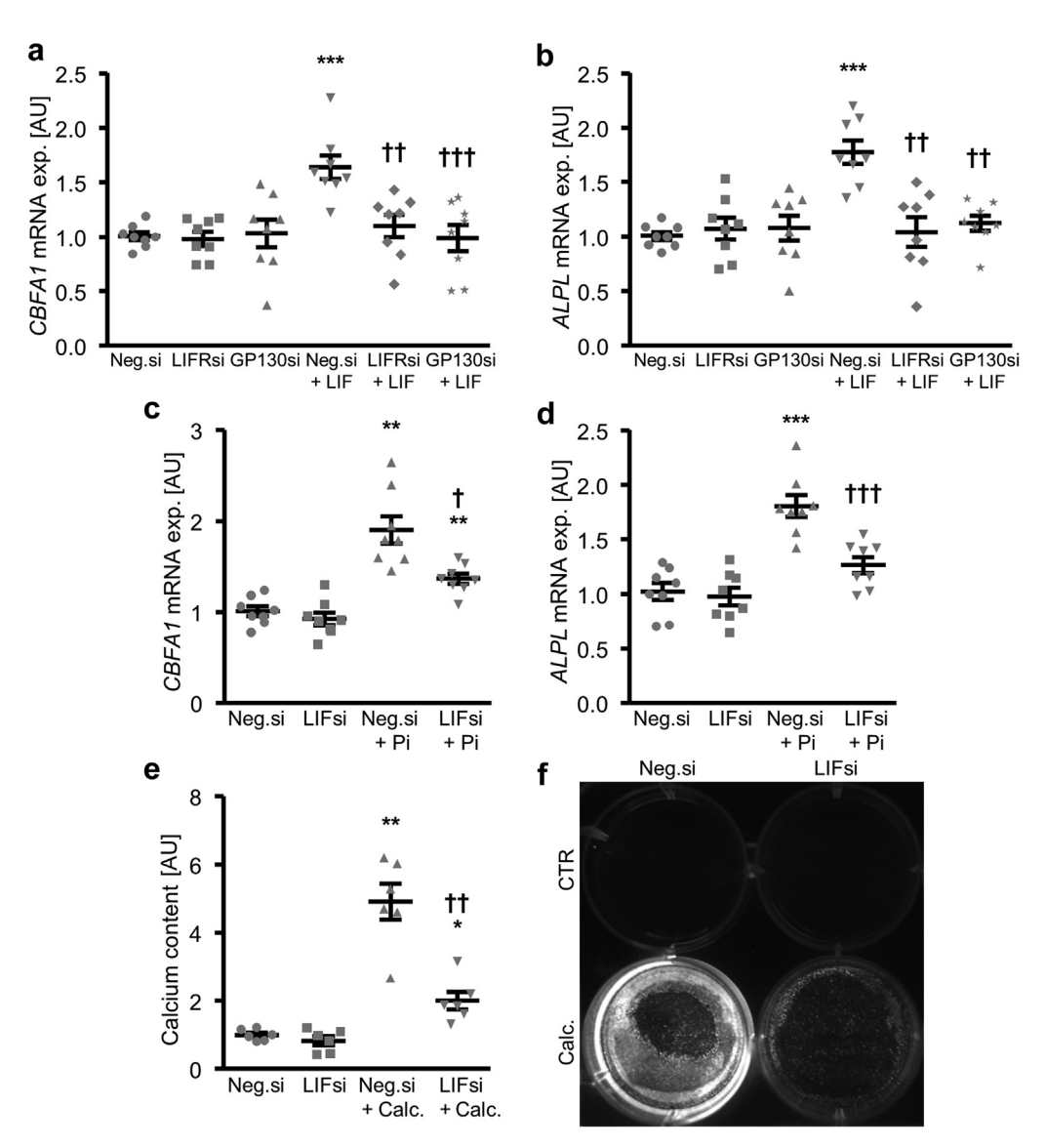


Figure 2 | Effects of leukemia inhibitory factor receptor (LIFR), glycoprotein 130 (GP130), and leukemia inhibitory factor (LIF) knockdown in procalcifying properties of vascular smooth muscle cells. Relative mRNA expression (exp.; n=8) of (a) *CBFA1* and (b) *ALPL* in human aortic smooth muscle cells (HAoSMCs) transfected with negative control (Neg.), LIFR, or GP130 small interfering RNA (siRNA; ie, Neg.si, LIFRsi, and GP130si) and treated for 24 hours with/without recombinant human LIF protein. ***P < 0.001 versus Neg.si; ††P < 0.01, ††P < 0.001 versus Neg.si + LIF (1-way analysis of variance [ANOVA] with Tukey honestly significant difference [HSD] test for [a] and with Games-Howell test for [b]). Relative mRNA expression (n = 8) of (c) *CBFA1* and (d) *ALPL* in HAoSMCs transfected with Neg. or LIF siRNA and treated for 24 hours with/without β-glycerophosphate (Pi). (e) Normalized calcium content (n = 6) and (f) calcification detected by Osteosense fluorescence imaging in HAoSMCs transfected with Neg. or LIF siRNA and treated for 11 days with/without calcification medium (Calc.). Calcified areas: white pseudocolor. **P < 0.01, ***P < 0.001 versus Neg.si; †P < 0.05, †P < 0.01, ††P < 0.001 versus Neg.si + Calc./Pi (1-way ANOVA with Games-Howell test for [c] and [e] and with Tukey-HSD test for [d]). AU, arbitrary unit; CTR, control.

Figure S15). Further experiments addressed TYK2 as a mediator of VSMC calcification, where TYK2 inhibition by BMS-986165 was able to reduce calcification of VSMCs (Figure 5h and i).

TYK2 was overexpressed in VSMCs to further extend on its critical role during VC (Supplementary Figure S16). TYK2 overexpression was sufficient to upregulate *CBFA1* and *ALPL* mRNA expression in VSMCs (Figure 6a and b) as well as calcification of VSMCs (Figure 6a–d). In turn, knockdown (Supplementary Figure S17) of either TYK2 (Figure 6e and f) or STAT3 (Figure 6g and h) again blunted the upregulation of

CBFA1 and ALPL mRNA expression induced by phosphate in VSMCs. STAT1 appeared to be also involved in the effects of phosphate, as similar observations were made after STAT1 silencing in VSMCs (Supplementary Figure S18). The role of the JAK-STAT pathway was further confirmed by treating VSMCs with the JAK inhibitors tofacitinib and ruxolitinib. These interfered with the upregulation of CBFA1 and ALPL mRNA expression induced by LIF, as well as after phosphate treatment (Supplementary Figure S19A–D). In the absence of triggers, CBFA1 or ALPL expression was not significantly modified by the JAK inhibitors (Supplementary Figure S19E and F).

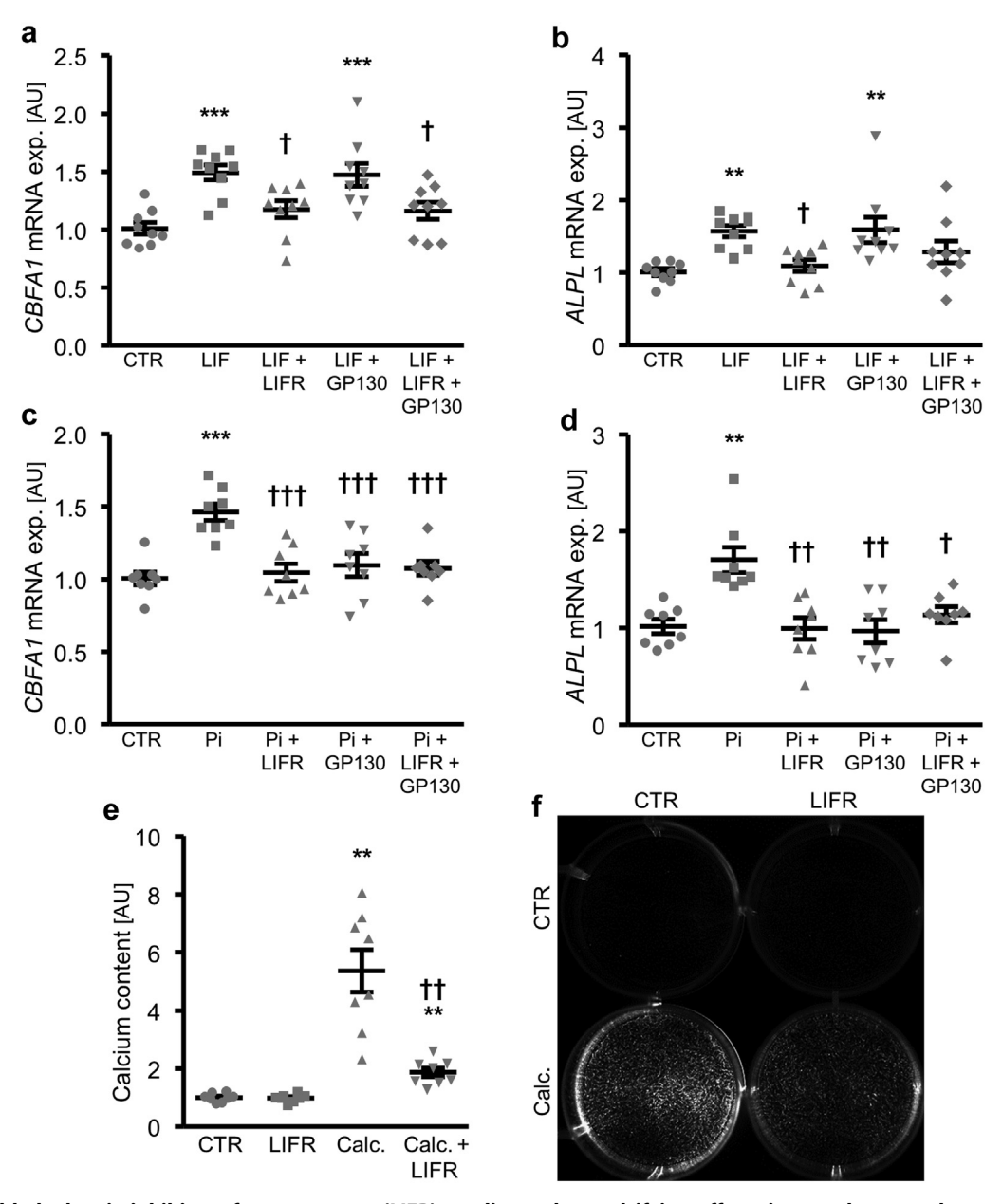


Figure 3 | Soluble leukemia inhibitory factor receptor (LIFR) ameliorated procalcifying effects in vascular smooth muscle cells. Relative mRNA expression (exp.; n=9) of (a) *CBFA1* and (b) *ALPL* in human aortic smooth muscle cells (HAoSMCs) treated for 24 hours with recombinant human leukemia inhibitory factor (LIF) protein with/without recombinant human LIFR or glycoprotein 130 (GP130) proteins. **P < 0.01, ***P < 0.01 versus control (CTR); †P < 0.05 versus LIF (1-way analysis of variance [ANOVA] with Tukey honestly significant difference [HSD] test for [a] and Kruskal-Wallis with Steel-Dwass test for [b]). Relative mRNA expression (n=8) of (c) *CBFA1* and (d) *ALPL* in HAoSMCs treated for 24 hours with β -glycerophosphate (Pi) with/without recombinant human LIFR or GP130 proteins. (e) Normalized calcium content (n=8) and (f) calcification detected by Osteosense fluorescence imaging in HAoSMCs treated for 11 days with calcification medium (Calc.) with/without recombinant human LIFR protein. Calcified areas: white pseudocolor. **P < 0.01, ***P < 0.001 versus CTR; †P < 0.05, ††P < 0.01, ††P < 0.001 versus Calc./Pi (1-way ANOVA with Tukey-HSD test for [c] and with Games-Howell test for [e] and Kruskal-Wallis with Steel-Dwass test for [d]). AU, arbitrary unit.

Further experiments (Supplementary Figure S20) addressed the functional role of this pathway in primary HObs. LIF increased *CBFA1* and *ALPL* mRNA expression and calcium deposition in calcifying HObs. However, TYK2 inhibition by BMS-986165 did not alter *CBFA1* or *ALPL* mRNA expression and rather increased the mineralization of HObs. Accordingly, BMS-986165 did not interfere with the LIF-

induced increase of *CBFA1* or *ALPL* mRNA expression in HObs (Supplementary Figure S20).

TYK2 inhibition ameliorated VC ex vivo and in vivo

Further experiments aimed to translate the protective effects of TYK2 blockade to vascular tissue. Aortic rings were isolated from mice and treated with phosphate in the presence of

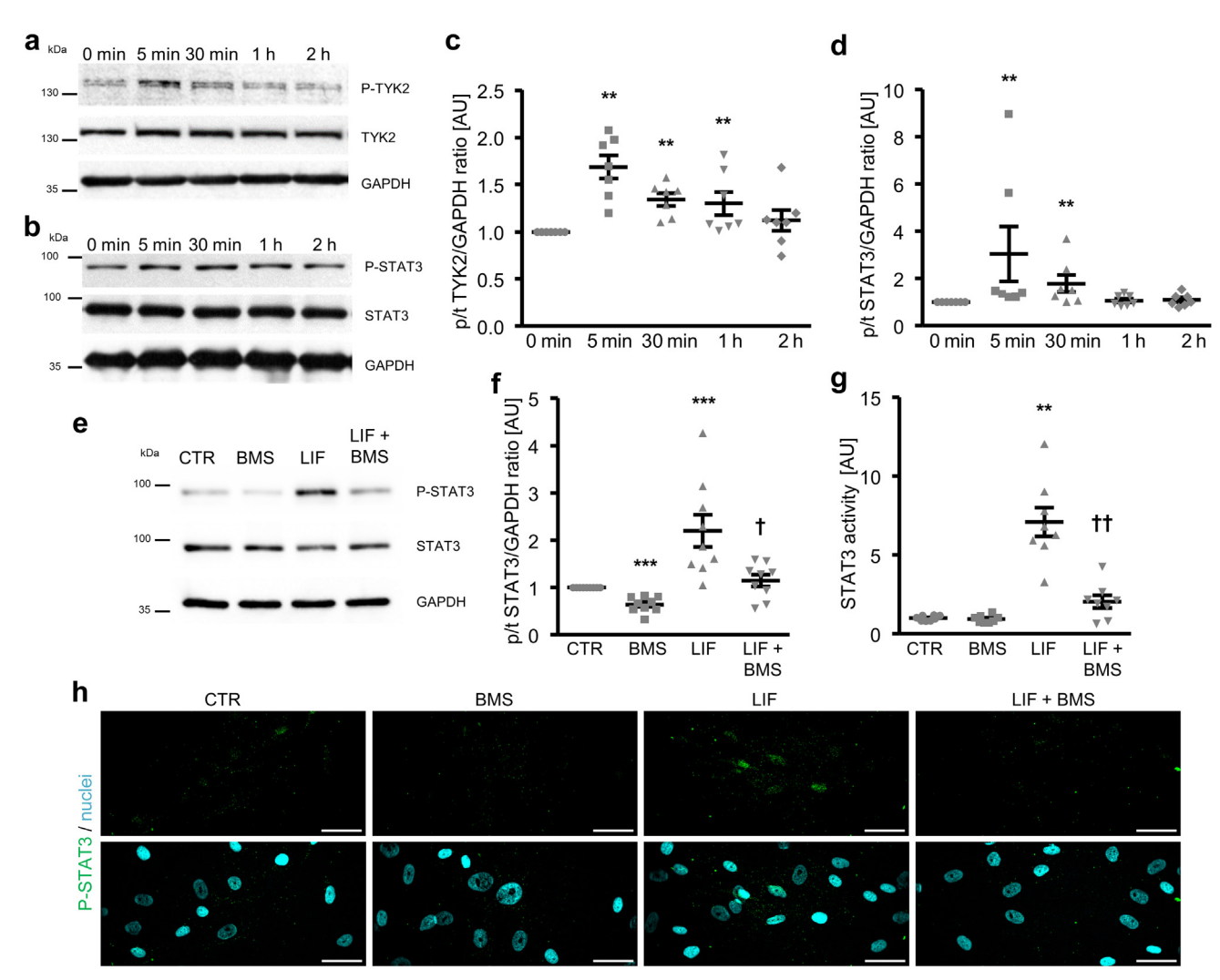


Figure 4 | Leukemia inhibitory factor (LIF)-induced tyrosine-protein kinase 2 (TYK2)-signal transducer and activator of transcription (STAT) activation in vascular smooth muscle cells. (a,b) Representative Western blots and normalized (c) phosphorylated TYK2 (P-TYK2) and (d) phosphorylated STAT3 (P-STAT3) protein abundance (n = 7) in human aortic smooth muscle cells (HAoSMCs) treated for the indicated times (0–2 hours) with recombinant human LIF protein. **P < 0.01 versus control (CTR; Kruskal-Wallis with Steel-Dwass test for [c,d]). (e) Representative Western blots and (f) normalized P-STAT3 protein abundance (n = 9) as well as (g) normalized STAT3 activity (n = 8) in HAoSMCs treated for 5 minutes with recombinant human LIF protein and with/without BMS-986165 (BMS). **P < 0.01, ***P < 0.01 versus CTR; †P < 0.05, ††P < 0.01 versus LIF (Kruskal-Wallis with Steel-Dwass test for [f] and 1-way analysis of variance with Games-Howell test for [g]). (h) P-STAT3 (green) and nuclei (blue) shown by confocal imaging in HAoSMCs treated for 30 minutes with recombinant human LIF protein and with/without BMS. Bar = 50 μ m. AU, arbitrary unit; GAPDH, glyceraldehyde-3-phosphate dehydrogenase; p/t, phosphorylated/total. To optimize viewing of this image, please see the online version of this article at www.kidney-international.org.

BMS-986165. Similarly, aortic rings from Tyk2-deficient mice and corresponding wild-type mice were treated with phosphate. As a result, either treatment with BMS-986165 or Tyk2 deficiency was able to reduce VC in aortic explants (Figure 7a–d; Supplementary Figure S21). Furthermore, the phosphate-induced increase of *Cbfa1* and *Alpl* mRNA expression was abrogated by pharmacologic Tyk2 inhibition or Tyk2 deficiency (Figure 7e–h).

To validate these protective effects *in vivo*, mice were treated with high-dosed cholecalciferol to induce VC. Cholecalciferol upregulated both *Lif* and *Lifr* mRNA expression in the aortic tissue (Figure 8a and b) and reduced the

levels of circulating Lifr in the serum (Supplementary Figure S22). Cholecalciferol treatment induced aortic calcification in mice, which was ameliorated by cotreatment with BMS-986165 (Figure 8c and d). In addition, the upregulation of *Cbfa1* and *Alpl* mRNA expression in the aortic tissue after cholecalciferol treatment was reduced after pharmacologic Tyk2 inhibition (Figure 8e and f). Cholecalciferol treatment further increased the aortic abundance of phosphorylated Stat3, an effect again blunted by BMS-986165 (Figure 8g). However, treatment with BMS-986165 also reduced the elevated serum concentrations of calcium after cholecalciferol treatment in mice, without strongly affecting serum

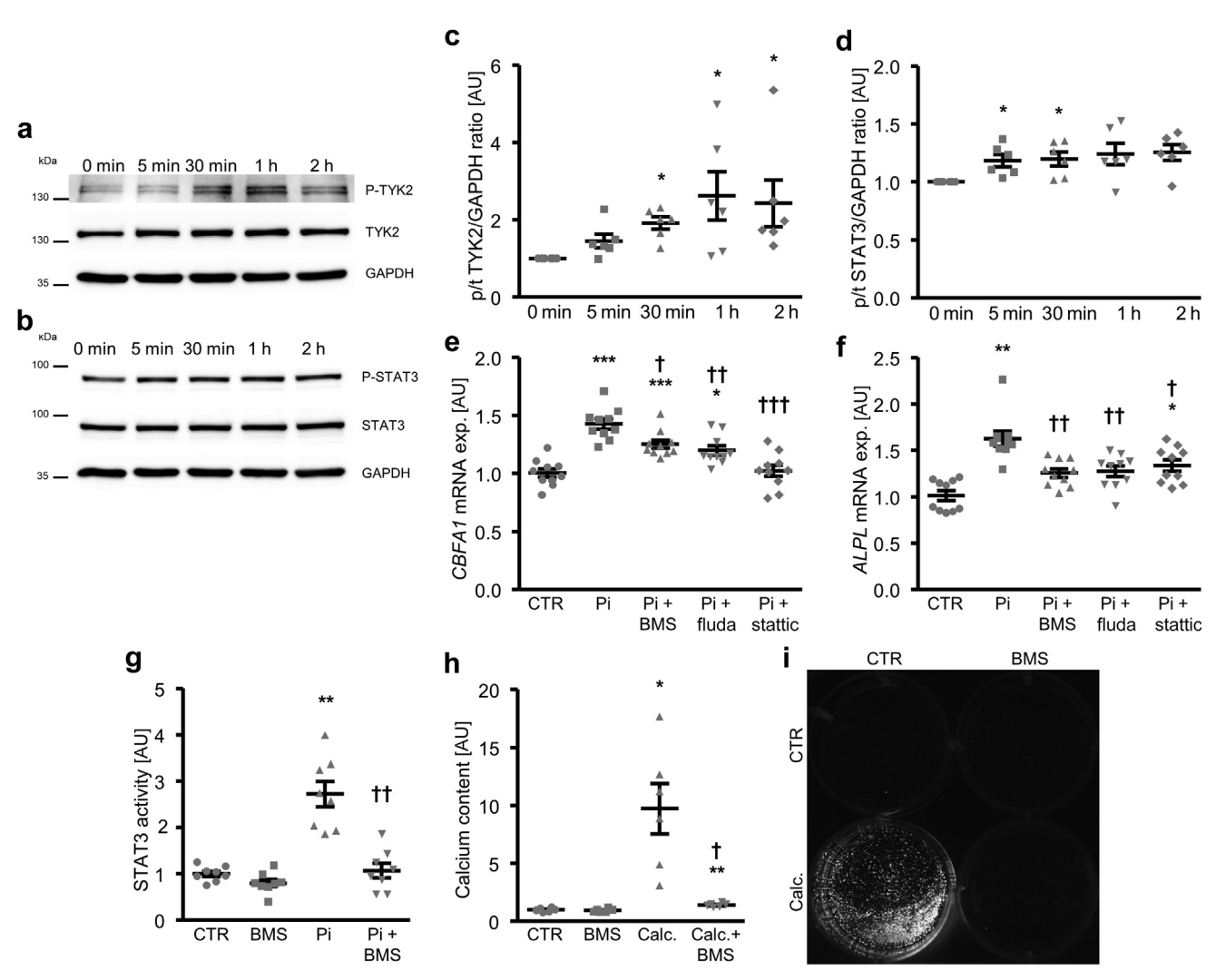


Figure 5 | Effects of tyrosine-protein kinase 2 (TYK2)-signal transducer and activator of transcription (STAT) pathway inhibition on phosphate-induced calcification of vascular smooth muscle cells. (a,b) Representative Western blots and normalized (c) phosphorylated TYK2 (P-TYK2) and (d) phosphorylated STAT3 (P-STAT3) protein abundance (n = 6) in human aortic smooth muscle cells (HAoSMCs) treated for the indicated times (0–2 hours) with β -glycerophosphate (Pi). *P < 0.05 versus control (CTR; Kruskal-Wallis with Steel-Dwass test for [c,d]). Relative mRNA expression (exp.; n = 10) of (e) *CBFA1* and (f) *ALPL* in HAoSMCs treated for 24 hours with control or Pi with/without BMS-986165 (BMS), fludarabine (fluda), or stattic. (g) Normalized STAT3 activity (n = 8) as well as (h) normalized calcium content (n = 6) and calcification detected by (i) Osteosense fluorescence imaging in HAoSMCs treated for 30 minutes and 11 days, respectively, with Pi/calcification medium (Calc.) and with/without BMS. Calcified areas: white pseudocolor. *P < 0.05, *P < 0.01, *P < 0.01, *P < 0.001 versus CTR; †P < 0.05, *P < 0.01, *P < 0.01, *P < 0.001 versus Pi/Calc. (1-way analysis of variance with Tukey honestly significant difference test for [e] and with Games-Howell test for [g,h] and Kruskal-Wallis with Steel-Dwass test for [f]). AU, arbitrary unit; GAPDH, glyceraldehyde-3-phosphate dehydrogenase; p/t, phosphorylated/total.

phosphate levels (Supplementary Table S1). In Tyk2-deficient mice, aortic calcification and mRNA expression of *Cbfa1* and *Alpl* were ameliorated on cholecalciferol treatment (Figure 8h–k), without alterations of serum calcium and phosphate levels (Supplementary Table S2).

To confirm the *in vivo* findings in a CKD mouse model, kidney failure was induced by treatment with an adenine/high-phosphorus diet in Abcc6-deficient and wild-type or Tyk2-deficient mice. This resulted in increased blood urea nitrogen levels in both genotypes; further serum biochemistry is shown in Supplementary Table S3. CKD mice had increased aortic *Lif* mRNA expression (Figure 9a),

without significant changes in aortic *Lifr* mRNA levels (Figure 9b). More important, the aortic calcium deposition and mRNA expression of osteogenic markers *Cbfa1* and *Alpl* induced by the adenine/high-phosphorus treatment were all suppressed by Tyk2 deficiency (Figure 9c–e). As the measurements of serum C-terminal telopeptide of type I collagen (CTX-I) and N-terminal propeptide of type I procollagen (PINP) markers indicated higher bone turnover in the adenine/high-phosphorus—treated mice (Supplementary Table S3), femora of these mice were analyzed by micro—computed tomography. In Tyk2-deficient mice treated with adenine/high phosphorus,

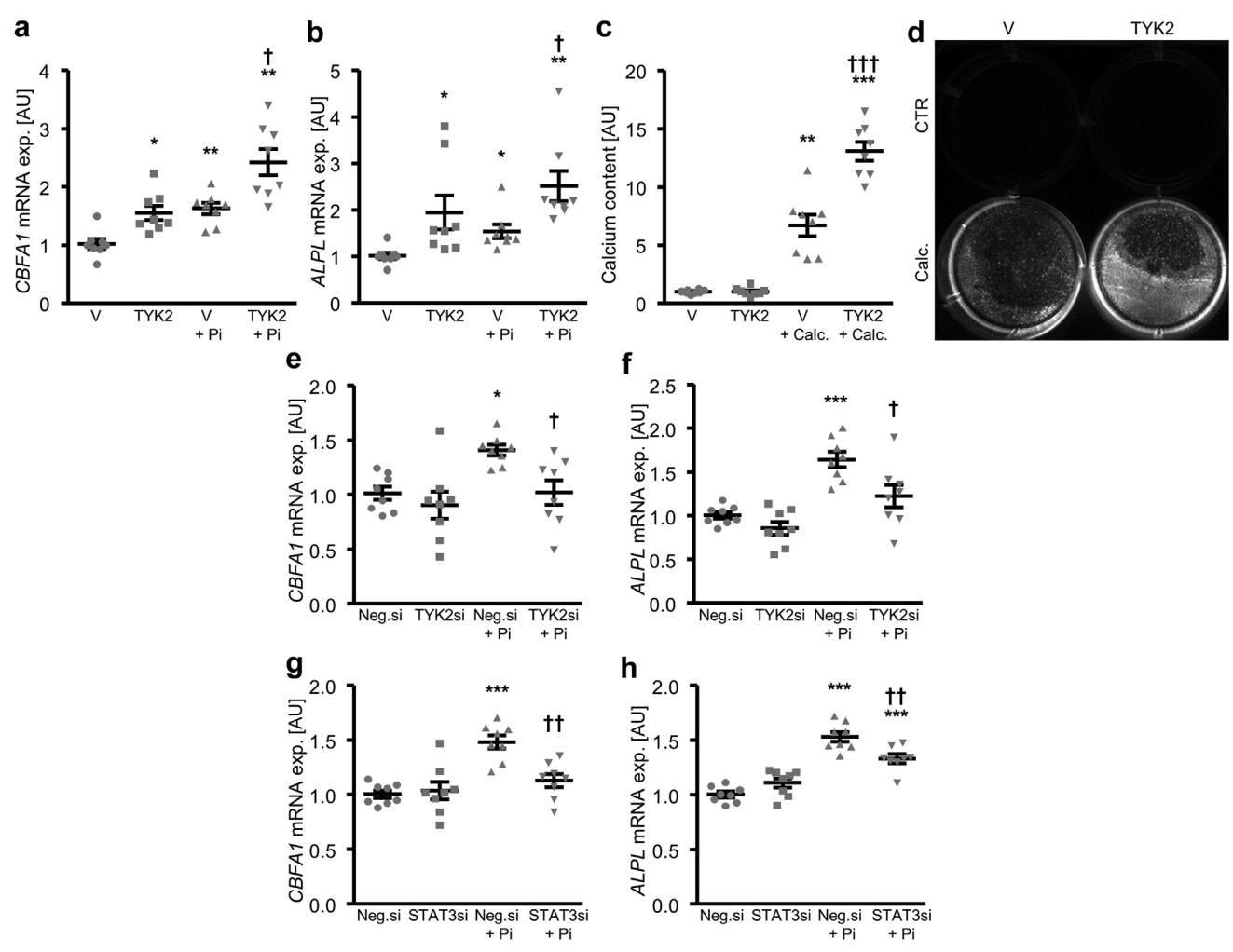


Figure 6 | Effects of tyrosine-protein kinase 2 (TYK2) overexpression and knockdown in phosphate-treated vascular smooth muscle cells. Relative mRNA expression (exp.; n=8) of (a) *CBFA1* and (b) *ALPL* as well as (c) normalized calcium content (n=8) and (d) calcification detected by Osteosense fluorescence imaging in human aortic smooth muscle cells (HAoSMCs) transfected with empty vector (V) or a construct encoding human TYK2 and treated for 24 hours and 11 days, respectively, with/without β-glycerophosphate (Pi)/calcification medium (Calc). Relative mRNA expression of *CBFA1* and *ALPL* in HAoSMCs transfected with (e,f) negative control (Neg.) and TYK2 (n=8) or (g,h) STAT3 (n=8) small interfering RNA (siRNA; ie, Neg.si, TYK2si, and STAT3si) and treated for 24 hours with/without Pi. *P<0.05, **P<0.01, ***P<0.01, ***P<0.01 versus Neg.si/V; P<0.05, *†P<0.05, *†P<0.01, *††P<0.01 versus Neg.si/V + Pi/Calc. (1-way analysis of variance with Games-Howell test for [a,c] and with Tukey honestly significant difference test for [e-h] and Kruskal-Wallis with Steel-Dwass test for [b]). AU, arbitrary unit; CTR, control.

cortical porosity was lower and bone mineral density was higher than in wild-type mice (Figure 9f–k). Trabecular separation was higher in Tyk2-deficient mice, but trabecular thickness and bone volume/total volume were not significantly altered.

DISCUSSION

This study describes a procalcific effect of LIF through the LIFR-GP130 complex in VSMCs. The mechanistic experiments identify TYK2 as a decisive regulator of procalcific STAT signaling and feasible therapeutic target in VC. Because multiple procalcific mediators involve activation of the STAT pathway, ^{7,11,12} inhibition of TYK2 might be a more potent and feasible therapeutic target than targeting procalcific mediators individually.

The IL-6 family member LIF is associated with pleiotropic effects, depending on cell type and developmental stage. ¹⁶ Both anti-inflammatory and pro-inflammatory effects are connected with LIF. ³³ In the vasculature, LIF has been linked to antiatherosclerotic effects. ²¹ Here, LIF may enhance the cholesterol uptake in the liver, ³⁴ and its primary effects may, thus, be extravascular. In ankylosing spondylitis, LIF is upregulated and exerts a procalcific effect in osteoblastic cells via upregulation of alkaline phosphatase. ³⁵ Lifdeficient mice exhibit a low trabecular bone mass. ³⁶ The procalcific effects of LIF might be concomitant with its wound-resolving and profibrotic functions. ²⁵ But the diverse effects of LIF are somehow in contrast to the more pro-inflammatory effects of IL-6, which is a known inducer of VC and atherosclerosis. ⁸ Nonetheless, LIF appears as another relevant

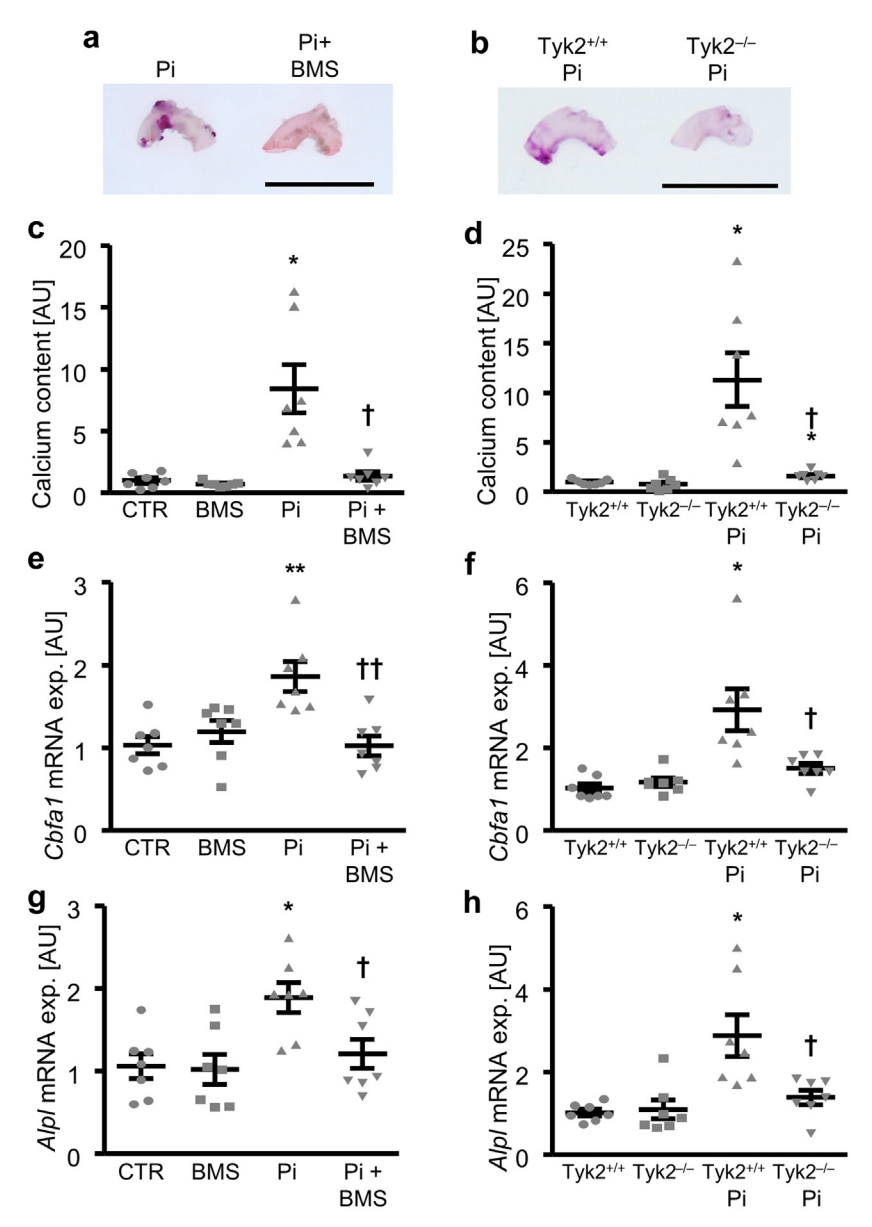


Figure 7 | Effects of tyrosine-protein kinase 2 (Tyk2) inhibition and deficiency ex vivo in calcifying mouse aortic explants. Alizarin red staining of mouse aortic arches (a) treated for 7 days with phosphate (Pi) with/without BMS-986165 (BMS) or (b) isolated from Tyk2-deficient (Tyk2 $^{-/-}$) and corresponding wild-type mice (Tyk2 $^{+/+}$). Calcification: red staining. Bar = 5 mm. (c,d) Normalized calcium content and relative mRNA expression of (e,f) Cbfa1 and (g,h) Alpl in mouse aortic tissue treated for 7 days with Pi with/without BMS (n = 7) or isolated from Tyk2 $^{-/-}$ and corresponding wild-type mice (Tyk2 $^{+/+}$; n = 7). *P < 0.05, **P < 0.01 versus control (CTR); †P < 0.05, †P < 0.01 versus Pi (Kruskal-Wallis with Steel-Dwass test for [c,f,h] and 1-way analysis of variance with Games-Howell test for [d] and with Tukey honestly significant different test for [e,g]). AU, arbitrary unit. To optimize viewing of this image, please see the online version of this article at www.kidney-international.org.

component orchestrating the procalcific alterations in the vasculature.

In VSMCs, the concerted effects of the IL-6 family members may be linked by their intracellular signaling pathways. LIF signals its calcific effects through the STAT pathway, involving STAT3 and additionally a role for STAT1. Although multiple other intracellular pathways are described, the STAT3 pathway is shared by IL-6 and oncostatin M, and both are able to promote VC.^{7,11} STAT3 could upregulate CBFA1 expression by enhancing transcription, which directly links STAT3 to VC.¹¹ In addition, STAT1 is phosphorylated in

response to LIE.¹⁵ STAT1 is also linked to CBFA1 expression and has recently been suggested as a putative signaling molecule in phosphate-induced VSMC calcification.^{37,38} However, this procalcific pathway is not limited to mediate the effects of IL-6 family members, but extends to other signaling molecules.¹² Phosphate exposure itself leads to activation of the STAT3 pathway in VSMCs, hypothetically through autocrine and paracrine effects of transmitter release from VSMCs. Silencing and inhibitory experiments of the LIF-STAT pathway indicate a prominent role for LIF in the activation of STAT-dependent calcification pathways in

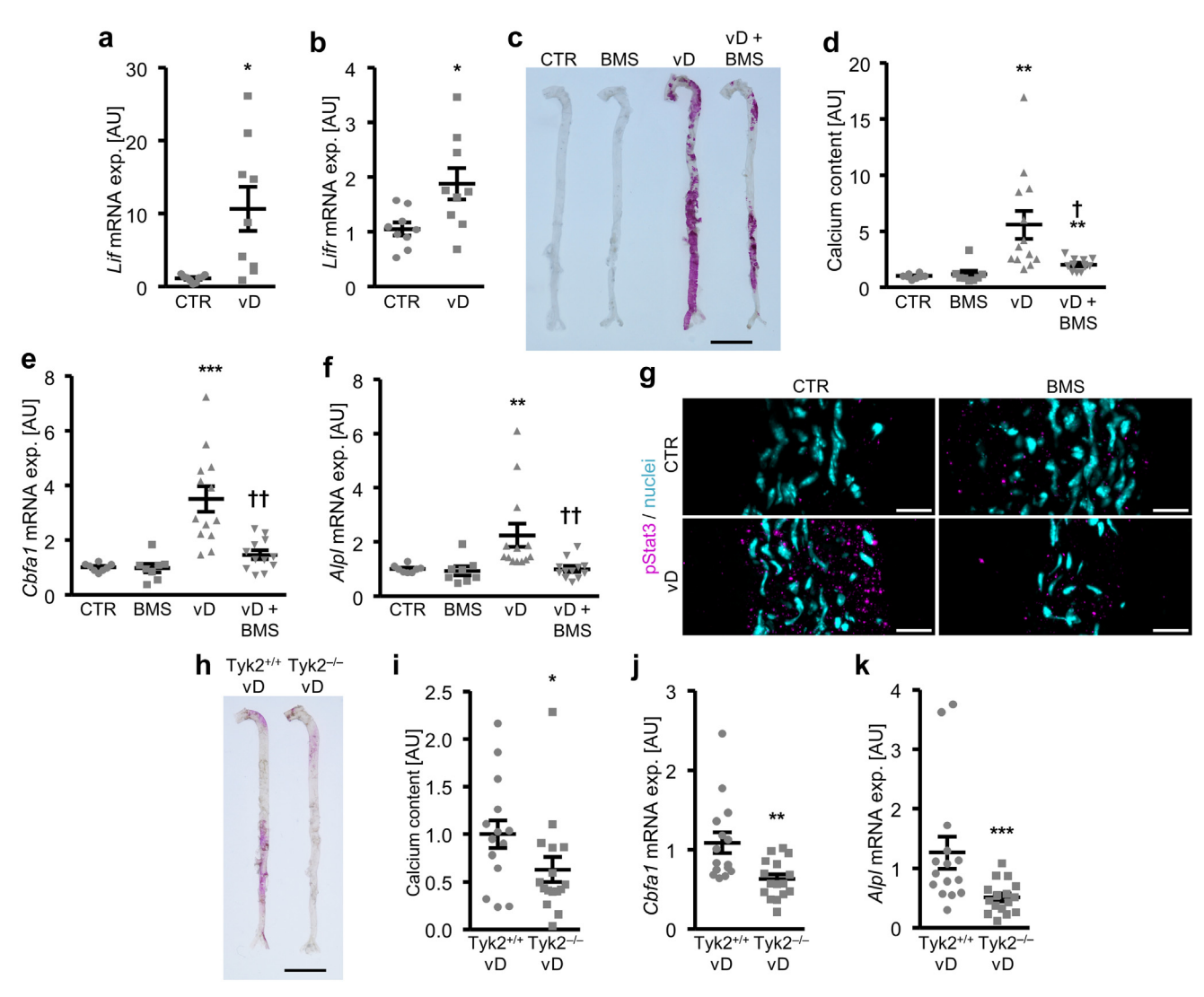


Figure 8 | Effects of tyrosine-protein kinase 2 (Tyk2) inhibition and deficiency in vivo during cholecalciferol overload. Relative aortic mRNA expression (exp.; n=9) of (a) Lif and (b) Lifr in mice treated without (control [CTR]) or with cholecalciferol (vD). (c) Alizarin red staining (calcification: red staining; bar = 5 mm), (d) normalized calcium content (n=8-13), relative mRNA expression (n=8-13) of (e) Cbfa1 and (f) Alpl, and (g) confocal imaging showing phosphorylated Stat3 (pStat3; green) and nuclei (blue; bar = 20 μ m) in aortic tissue of mice treated without (CTR) or with cholecalciferol (vD) and with/without BMS-986165 (BMS). (h) Alizarin red staining (calcification: red staining; bar = 5 mm), (i) normalized calcium content (n=15-16), and relative mRNA expression (n=15-16) of (j) Cbfa1 and (k) Alpl in aortic tissue of Tyk2-deficient (Tyk2^{-/-}) and corresponding wild-type mice (Tyk2^{+/+}) treated with cholecalciferol (vD). *P < 0.05, **P < 0.01, ***P < 0.001 versus CTR/Tyk2^{+/+} + vD; †P < 0.05, †P < 0.01 versus vD (unpaired 2-tailed t test for [a,b], Mann-Whitney U test for [i-k], Kruskal-Wallis with Steel-Dwass test for [d,f], and 1-way analysis of variance with Games-Howell test for [e]). AU, arbitrary unit. To optimize viewing of this image, please see the online version of this article at www.kidney-international.org.

VSMCs on phosphate exposure. In theory, LIF could induce this procalcific pathway even under conditions of IL-6 inhibition and hamper its protective effects in VC.

In the context of VC, especially the understudied upstream regulators of the STAT pathway appear to be of therapeutic relevance. We identified the kinase TYK2, a member of the Janus family of protein tyrosine kinases, as an essential component of the LIF response and the procalcific STAT pathway. The involvement of JAK-dependent signaling in these effects is further confirmed by the JAK1/2 inhibitor ruxolitinib and the JAK1/3 inhibitor tofacitinib. TYK2 is associated with interferon and

interleukin receptors.¹⁴ Suggesting a functional role in the vasculature, TYK2 was shown upregulated in rat carotid arteries after balloon injury³⁹ and phosphorylated in VSMCs after angiotensin II exposure.⁴⁰ In VSMCs, the effects of urokinase involve TYK2.^{14,41} Urokinase induces pro-inflammatory effects via a TYK2/STAT3 pathway in mesangial cells,⁴² and urokinase augments calcification in mesenchymal stem cells.⁴³ A critical role for TYK2 in cardiovascular calcification is supported by procalcific effects of several upstream activators, such as interferon⁴⁴ and oncostatin M.⁷ But although LIF induces TYK2 and STAT3, all functionally relevant in VC, the involvement of

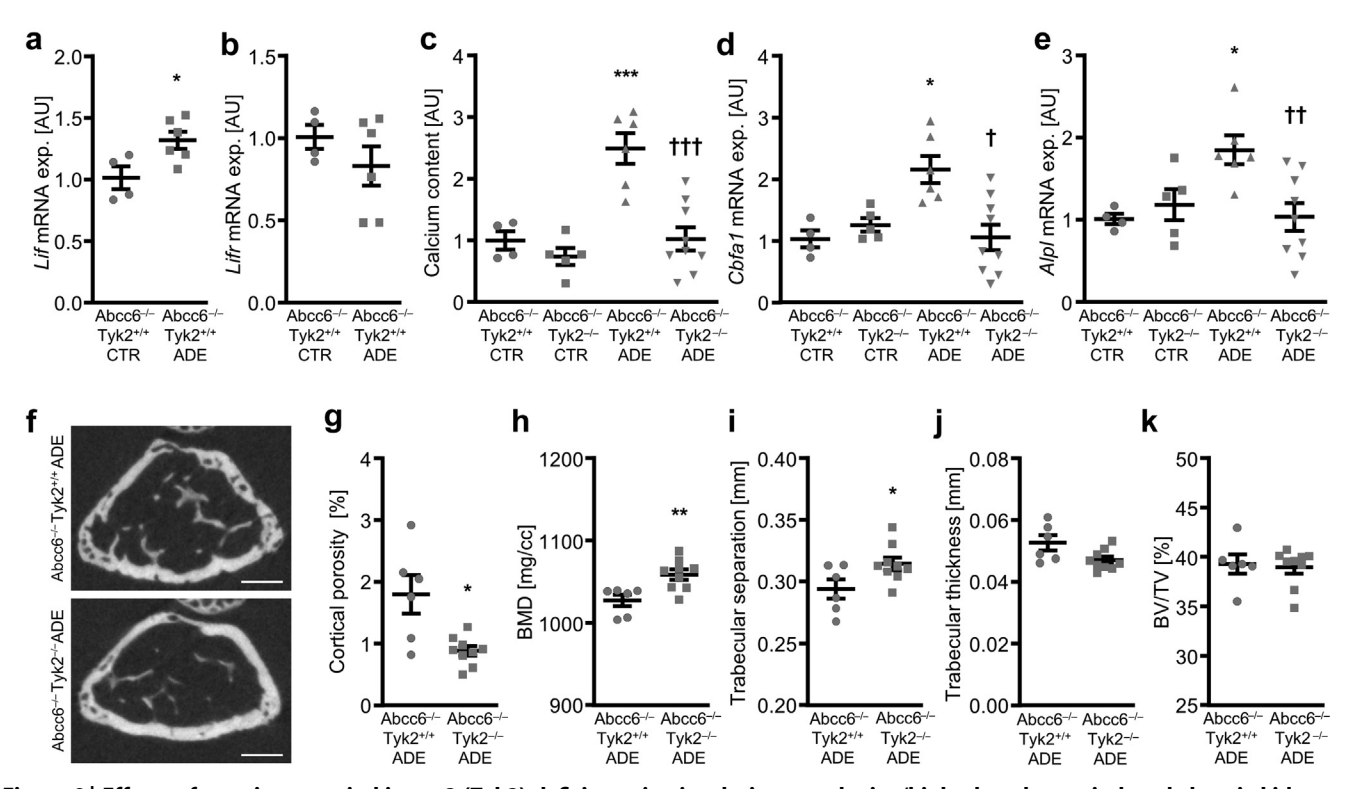


Figure 9 | Effects of tyrosine-protein kinase 2 (Tyk2) deficiency *in vivo* during an adenine/high-phosphorus-induced chronic kidney disease model in ATP-binding cassette subfamily C member 6 (Abcc6)-deficient mice. Relative aortic mRNA expression (exp.; n = 4-6) of (a) *Lif* and (b) *Lifr* in Abcc6-deficient (Abcc6-/-) Tyk2 wild-type (Tyk2+/+) mice treated with control (CTR) or adenine/high phosphorus (ADE). (c) Normalized calcium content (n = 4-9) and relative mRNA expression (n = 4-9) of (d) *Cbfa1* and (e) *Alpl* in aortic tissue of Abcc6-/- and Tyk2-deficient (Tyk2-/-) or corresponding wild-type (Tyk2+/+) mice treated with CTR or ADE. *P < 0.05, ***P < 0.001 versus Abcc6-/- Tyk2+/+ ADE (unpaired 2-tailed t test for [a,b], 1-way analysis of variance [ANOVA] with Tukey honestly significant difference test for [c,e], and 1-way ANOVA with Games-Howell test for [d). (f) Representative micro-computed tomography images (bar = 500 µm), (g) cortical porosity, (h) bone mineral density (BMD), (i) trabecular separation, (j) trabecular thickness, and (k) bone volume/total volume (BV/TV) from distal femora (n = 6-9) of Abcc6-/- and Tyk2-/- or corresponding wild-type (Tyk2+/+) mice treated with ADE. *P < 0.05, **P < 0.01 versus Abcc6-/- Tyk2+/+ ADE (unpaired 2-tailed t test for [g,i,j], and Mann-Whitney t test for [h,k]). AU, arbitrary unit. To optimize viewing of this image, please see the online version of this article at www.kidney-international.org.

other signaling pathways in this cascade cannot be ruled out. 16

The current observations also suggest that the role of TYK2 in VSMCs extends beyond the effects of LIF, as TYK2 inhibition strongly interferes with VC in the absence of exogenous LIF supplementation. This could be due to inhibition of effects from endogenous produced LIF, but also other autocrine/paracrine mediators released from calcifying VSMCs. Furthermore, TYK2 inhibition by BMS-986165 ameliorates VC in vivo, suggesting a therapeutic potential. Surprisingly, BMS-986165 alters serum calcium levels in cholecalciferol-treated mice. This could be due to an off-target effect on other kinases despite the selectivity profile. Nonetheless, ex vivo experiments and experiments in Tyk2-deficient mice clearly indicate a direct vascular effect of TYK2, independent of systemic mineral metabolism regulation. However, the current observations cannot rule out a direct or indirect role for TYK2 in calcium-phosphate metabolism or kidney injury. TYK2 could affect calcium and phosphate levels by alterations in bone metabolism during CKD, as Tyk2 deficiency lowers cortical porosity in adenine/high-phosphorus-treated mice. Cortical porosity is a hallmark of bone disorder in CKD and is discussed as a critical factor determining fracture risk. 45,46 This is also reflected in phosphate-fed mice with CKD, which exhibit increased cortical porosity together with reduced trabecular separation.⁴⁷ In the Abcc6 deficiency-adenine/high-phosphorus mouse model, Tyk2 deficiency appears to improve these alterations in bone. Various components of the JAK/STAT pathway have rather diverse and complex effects on bone remodeling, where the role of TYK2 is not well established.⁴⁸ The mechanisms underlying the altered bone dynamics in Tyk2 deficiency during CKD are currently unclear and could also involve other systemic effects. A protective role of Tyk2 in bone remodeling of CKD mice is somehow in contrast to the effects of LIF, which increases mineralization in both VSMCs and HObs. However, the effects of LIF on HObs are not sensitive to the TYK2 inhibitor BMS-986165, which rather promoted mineralization. Thus, the effects of LIF on osteoblasts appear to be mediated by a different pathway, not involving TYK2.

The importance of the STAT pathway in VC has been firmly established in preclinical research.^{3,38} The STAT pathways appear to integrate a variety of procalcific signals to promote VC.3 However, specific pharmacologic inhibition of STATs is challenging, and JAK inhibitors are under scrutiny for potentially dangerous adverse effects. 49,50 TYK2 inhibition has been developed to interfere with autoimmune pathways,⁵¹ and deucravacitinib has successfully been established for the treatment of psoriasis in humans.⁵² It has been argued that TYK2 inhibition has a more beneficial safety profile than other JAK inhibitors, also because Tyk2-deficient mice have a less severe phenotype than other Jak-deficient mice.⁵³ As multiple procalcific signals apparently converge on STAT signaling in VSMCs, its inhibition might be even more advantageous compared with blocking individual signaling molecules, such as LIF, interferon type I, 44 IL-29, 12 or IL-6 by ziltivekimab. 10 The current observations suggest that TYK2 inhibition might be a feasible and translatable strategy to reduce VC in CKD.

In conclusion, these results suggest a novel procalcific role of LIF in VSMCs. The signaling pathways mediating the effects of LIF identify TYK2 as a central regulator of phosphate-induced calcification of VSMCs. Inhibition of TYK2 is able to ameliorate VC *in vivo*. TYK2 deficiency ameliorates CKD-associated VC, but appears to improve bone alterations. Given its central role, safety profile, and availability, TYK2 inhibition by deucravacitinib could develop into a new and easily translatable strategy to reduce the burden of VC in patients with CKD.

DISCLOSURE

All the authors declared no competing interests.

DATA STATEMENT

The data supporting the findings of this study are available in the main manuscript or the Supplementary Material. In addition, we will share models, protocols, methods, and other useful materials and resources related to the article as far as possible. There are no large data files to be shared via online resources.

ACKNOWLEDGMENTS

The authors gratefully acknowledge the technical assistance of Dr. A. Sohail, I. Jannat, S. Shojaei, B. Moser, and F. Poetsch, as well as the support of Dr. S. Belenkov (Revvity) and P. Heimel (Ludwig Boltzmann Institute for Traumatology, The Research Center in Cooperation with AUVA) by conducting the micro–computed tomography analysis.

FUNDING STATEMENT

This work was funded by the Deutsche Forschungsgemeinschaft (VO2259/2-1) and the Austrian Science Fund (10.55776/P34724, 10.55776/F61). Open access funding was provided by the Austrian Science Fund.

AUTHOR CONTRIBUTIONS

JV and IA designed research and drafted the manuscript with comments and edits from all authors. IA, MR, TTDL, ME, LP, LAH, CD, and JV performed experiments. IA, MR, JO, GM, DZ, MS, CD, MMa, CG-T, AP, DC, SS, MA, BB, MMü;, AV, JH, K-UE, and JV analyzed and interpreted data and provided conceptual advice. All authors

discussed the results and approved the final version of the manuscript.

Supplementary material is available online at www.kidney-international.org.

REFERENCES

- Voelkl J, Cejka D, Alesutan I. An overview of the mechanisms in vascular calcification during chronic kidney disease. Curr Opin Nephrol Hypertens. 2019:28:289–296
- Voelkl J, Egli-Spichtig D, Alesutan I, Wagner CA. Inflammation: a putative link between phosphate metabolism and cardiovascular disease. Clin Sci (Lond). 2021:135:201–227.
- Voelkl J, Lang F, Eckardt KU, et al. Signaling pathways involved in vascular smooth muscle cell calcification during hyperphosphatemia. Cell Mol Life Sci. 2019;76:2077–2091.
- Cobb AM, Yusoff S, Hayward R, et al. Runx2 (runt-related transcription factor 2) links the DNA damage response to osteogenic reprogramming and apoptosis of vascular smooth muscle cells. Arterioscler Thromb Vasc Biol. 2021;41:1339–1357.
- Weng JJ, Su Y. Nuclear matrix-targeting of the osteogenic factor Runx2 is essential for its recognition and activation of the alkaline phosphatase gene. *Biochim Biophys Acta*. 2013;1830:2839–2852.
- Haarhaus M, Cianciolo G, Barbuto S, et al. Alkaline phosphatase: an old friend as treatment target for cardiovascular and mineral bone disorders in chronic kidney disease. *Nutrients*. 2022;14:2124.
- Kakutani Y, Shioi A, Shoji T, et al. Oncostatin M promotes osteoblastic differentiation of human vascular smooth muscle cells through JAK3-STAT3 pathway. J Cell Biochem. 2015;116:1325–1333.
- Henaut L, Massy ZA. New insights into the key role of interleukin 6 in vascular calcification of chronic kidney disease. Nephrol Dial Transplant. 2018;33:543–548.
- Roy N, Rosas SE. IL-6 is associated with progression of coronary artery calcification and mortality in incident dialysis patients. Am J Nephrol. 2021;52:745–752.
- Ridker PM, Devalaraja M, Baeres FMM, et al. IL-6 inhibition with ziltivekimab in patients at high atherosclerotic risk (RESCUE): a doubleblind, randomised, placebo-controlled, phase 2 trial. *Lancet*. 2021;397: 2060–2069.
- Kurozumi A, Nakano K, Yamagata K, et al. IL-6 and sIL-6R induces STAT3dependent differentiation of human VSMCs into osteoblast-like cells through JMJD2B-mediated histone demethylation of RUNX2. Bone. 2019:124:53–61.
- Hao N, Zhou Z, Zhang F, et al. Interleukin-29 accelerates vascular calcification via JAK2/STAT3/BMP2 signaling. J Am Heart Assoc. 2023;12: e027222.
- Xiang Y, Duan Y, Peng Z, et al. Microparticles from hyperphosphatemiastimulated endothelial cells promote vascular calcification through astrocyte-elevated gene-1. Calcif Tissue Int. 2022;111:73–86.
- Strobl B, Stoiber D, Sexl V, Mueller M. Tyrosine kinase 2 (TYK2) in cytokine signalling and host immunity. Front Biosci (Landmark Ed). 2011;16:3214– 3232.
- Jenab S, Morris PL. Testicular leukemia inhibitory factor (LIF) and LIF receptor mediate phosphorylation of signal transducers and activators of transcription (STAT)-3 and STAT-1 and induce c-fos transcription and activator protein-1 activation in rat Sertoli but not germ cells. Endocrinology. 1998;139:1883–1890.
- Nicola NA, Babon JJ. Leukemia inhibitory factor (LIF). Cytokine Growth Factor Rev. 2015;26:533–544.
- Lokau J, Garbers C. Biological functions and therapeutic opportunities of soluble cytokine receptors. Cytokine Growth Factor Rev. 2020;55:94–108.
- Zhang JG, Zhang Y, Owczarek CM, et al. Identification and characterization of two distinct truncated forms of gp130 and a soluble form of leukemia inhibitory factor receptor alpha-chain in normal human urine and plasma. *J Biol Chem.* 1998;273:10798–10805.
- Tomida M, Yamamoto-Yamaguchi Y, Hozumi M. Pregnancy associated increase in mRNA for soluble D-factor/LIF receptor in mouse liver. FEBS Lett. 1993;334:193–197.
- Wang J, Chang CY, Yang X, et al. Leukemia inhibitory factor, a doubleedged sword with therapeutic implications in human diseases. *Mol Ther*. 2023;31:331–343.

- Rolfe BE, Stamatiou S, World CJ, et al. Leukaemia inhibitory factor retards the progression of atherosclerosis. Cardiovasc Res. 2003;58:222–230.
- Moran CS, Campbell JH, Campbell GR. Induction of smooth muscle cell nitric oxide synthase by human leukaemia inhibitory factor: effects in vitro and in vivo. J Vasc Res. 1997;34:378–385.
- 23. Sims NA, Johnson RW. Leukemia inhibitory factor: a paracrine mediator of bone metabolism. *Growth Factors*. 2012;30:76–87.
- 24. Pollock JH, Blaha MJ, Lavish SA, et al. *In vivo* demonstration that parathyroid hormone and parathyroid hormone-related protein stimulate expression by osteoblasts of interleukin-6 and leukemia inhibitory factor. *J Bone Miner Res.* 1996;11:754–759.
- Xu S, Yang X, Chen Q, et al. Leukemia inhibitory factor is a therapeutic target for renal interstitial fibrosis. EBioMedicine. 2022;86:104312.
- Ciceri P, Bono V, Magagnoli L, et al. Cytokine and chemokine retention profile in COVID-19 patients with chronic kidney disease. *Toxins (Basel)*. 2022;14:673.
- Alesutan I, Luong TTD, Schelski N, et al. Circulating uromodulin inhibits vascular calcification by interfering with pro-inflammatory cytokine signalling. Cardiovasc Res. 2021;117:930–941.
- Voelkl J, Luong TT, Tuffaha R, et al. SGK1 induces vascular smooth muscle cell calcification through NF-kappaB signaling. J Clin Invest. 2018;128: 3024–3040.
- Luong TTD, Tuffaha R, Schuchardt M, et al. Acid sphingomyelinase promotes SGK1-dependent vascular calcification. Clin Sci (Lond). 2021;135:515–534.
- Vielnascher RM, Hainzl E, Leitner NR, et al. Conditional ablation of TYK2 in immunity to viral infection and tumor surveillance. *Transgenic Res*. 2014;23:519–529.
- Henze LA, Luong TTD, Boehme B, et al. Impact of C-reactive protein on osteo-/chondrogenic transdifferentiation and calcification of vascular smooth muscle cells. Aging (Albany NY). 2019;11:5445–5462.
- Poetsch F, Henze LA, Estepa M, et al. Role of SGK1 in the osteogenic transdifferentiation and calcification of vascular smooth muscle cells promoted by hyperglycemic conditions. *Int J Mol Sci.* 2020;21:7207.
- Knight D. Leukaemia inhibitory factor (LIF): a cytokine of emerging importance in chronic airway inflammation. *Pulm Pharmacol Ther*. 2001:14:169–176.
- Moran CS, Campbell JH, Campbell GR. Human leukemia inhibitory factor upregulates LDL receptors on liver cells and decreases serum cholesterol in the cholesterol-fed rabbit. Arterioscler Thromb Vasc Biol. 1997;17:1267– 1273
- Kong W, Tang Y, Tang K, et al. Leukemia inhibitory factor is dysregulated in ankylosing spondylitis and contributes to bone formation. *Int J Rheum Dis*. 2022;25:592–600.
- Poulton IJ, McGregor NE, Pompolo S, et al. Contrasting roles of leukemia inhibitory factor in murine bone development and remodeling involve region-specific changes in vascularization. J Bone Miner Res. 2012;27:586–595.
- Li P, Wang Y, Liu X, et al. Loss of PARP-1 attenuates diabetic arteriosclerotic calcification via Stat1/Runx2 axis. Cell Death Dis. 2020;11:22.

- Qin Z, Li Y, Li J, et al. Exosomal STAT1 derived from high phosphorusstimulated vascular endothelial cells induces vascular smooth muscle cell calcification via the Wnt/beta-catenin signaling pathway. *Int J Mol Med*. 2022;50:139.
- **39.** Seki Y, Kai H, Shibata R, et al. Role of the JAK/STAT pathway in rat carotid artery remodeling after vascular injury. *Circ Res.* 2000;87:12–18.
- Marrero MB, Schieffer B, Paxton WG, et al. Direct stimulation of Jak/STAT pathway by the angiotensin II AT1 receptor. *Nature*. 1995;375:247–250.
- Patecki M, von Schaewen M, Tkachuk S, et al. Tyk2 mediates effects of urokinase on human vascular smooth muscle cell growth. *Biochem Biophys Res Commun*. 2007;359:679–684.
- Shushakova N, Tkachuk N, Dangers M, et al. Urokinase-induced activation of the gp130/Tyk2/Stat3 pathway mediates a proinflammatory effect in human mesangial cells via expression of the anaphylatoxin C5a receptor. J Cell Sci. 2005;118(pt 12):2743–2753.
- Kalbasi Anaraki P, Patecki M, Larmann J, et al. Urokinase receptor mediates osteogenic differentiation of mesenchymal stem cells and vascular calcification via the complement C5a receptor. Stem Cells Dev. 2014;23:352–362.
- Parra-Izquierdo I, Castanos-Mollor I, Lopez J, et al. Calcification induced by type I interferon in human aortic valve interstitial cells is larger in males and blunted by a Janus kinase inhibitor. Arterioscler Thromb Vasc Biol. 2018:38:2148–2159.
- Drueke TB, Massy ZA. Changing bone patterns with progression of chronic kidney disease. Kidney Int. 2016;89:289–302.
- Nickolas TL, Stein EM, Dworakowski E, et al. Rapid cortical bone loss in patients with chronic kidney disease. J Bone Miner Res. 2013;28:1811– 1820
- Lau WL, Linnes M, Chu EY, et al. High phosphate feeding promotes mineral and bone abnormalities in mice with chronic kidney disease. Nephrol Dial Transplant. 2013;28:62–69.
- Damerau A, Gaber T, Ohrndorf S, Hoff P. JAK/STAT activation: a general mechanism for bone development, homeostasis, and regeneration. Int J Mol Sci. 2020;21:9004.
- 49. Hu X, Li J, Fu M, et al. The JAK/STAT signalling pathway: from bench to clinic. Signal Transduct Target Ther. 2021;6:402.
- Hoisnard L, Lebrun-Vignes B, Maury S, et al. Adverse events associated with JAK inhibitors in 126,815 reports from the WHO pharmacovigilance database. Sci Rep. 2022;12:7140.
- Burke JR, Cheng L, Gillooly KM, et al. Autoimmune pathways in mice and humans are blocked by pharmacological stabilization of the TYK2 pseudokinase domain. Sci Transl Med. 2019;11:eaaw1736.
- Armstrong AW, Gooderham M, Warren RB, et al. Deucravacitinib versus placebo and apremilast in moderate to severe plaque psoriasis: efficacy and safety results from the 52-week, randomized, double-blinded, placebo-controlled phase 3 POETYK PSO-1 trial. J Am Acad Dermatol. 2023;88:29–39.
- Muromoto R, Shimoda K, Oritani K, Matsuda T. Therapeutic advantage of Tyk2 inhibition for treating autoimmune and chronic inflammatory diseases. *Biol Pharm Bull*. 2021;44:1585–1592.